Molecular Crystals and Liquid Crystals Science and Technology. Section A. Molecular Crystals and Liquid Crystals

Publication details, including instructions for authors and subscription information:
http://www.tandfonline.com/loi/gmcl19

Novel Polymeric Materials, Architectures, and Characterization Techniques for Electro-Optics

Steffen Weiss [a], Wolfgang H. Meyer [a], Emil F. Aust [b c] & Wolfgang Knoll [b c]

[a] Max-Planck-Institut für Polymerforschung, Ackerraannweg 10, D-55128, Mainz, Germany

[b] Max-Planck-Institut für Polymerforschung, Ackermannweg 10, D-55128, Mainz, Germany

[c] The Institute of Physical and Chemical Research (RIKEN), 2-1 Hirosawa, Wako-shi, Saitama, 351-01, Japan

Version of record first published: 04 Oct 2006.

To cite this article: Steffen Weiss , Wolfgang H. Meyer , Emil F. Aust & Wolfgang Knoll (1996): Novel Polymeric Materials, Architectures, and Characterization Techniques for Electro-Optics, Molecular Crystals and Liquid Crystals Science and Technology. Section A. Molecular Crystals and Liquid Crystals, 280:1, 257-270

To link to this article: http://dx.doi.org/10.1080/10587259608040341

Mol. Cryst. Liq. Cryst., 1996, Vol. 280, pp. 257–270
Reprints available directly from the publisher
Photocopying permitted by license only

NOVEL POLYMERIC MATERIALS, ARCHITECTURES, AND CHARACTERIZATION TECHNIQUES FOR ELECTRO-OPTICS[§]

STEFFEN WEISS, WOLFGANG H. MEYER
Max-Planck-Institut für Polymerforschung, Ackermannweg 10, D-55128 Mainz, Germany

EMIL F. AUST, WOLFGANG KNOLL
Max-Planck-Institut für Polymerforschung, Ackermannweg 10, D-55128 Mainz, Germany, and Frontier Research Program, The Institute of Physical and Chemical Research (RIKEN), 2-1 Hirosawa, Wako-shi, Saitama 351-01, Japan

Abstract This contribution deals with recent developments in the field of integrated electro-optics. We first present a novel characterization technique based on optical waveguide microscopy that allows for the imaging of linear and nonlinear optical lateral heterogeneities in planar waveguide structures. Next, a new class of amorphous polymers is introduced: the charged groups of solid polyelectrolytes are compensated by counter-ions with a high $\chi^{(2)}$ response. The advantage of these materials is their high level of doping that can be achieved without recrystallization observed for other host/ guest-systems. And finally, we present waveguide structures based on the Langmuir/ Blodgett/ Kuhn-technique with a complex internal optical architecture controlled at the molecular level.

INTRODUCTION

The aim of our research in the field of organic photonic materials is threefold: 1) We are interested in a general improvement of the structural and functional properties of existing polymers and of new systems; 2) we see the need for the development for additional experimental techniques that allow for a detailed analysis of these materials, their properties and performance and 3) we would like to derive to a better understanding of the relation between the microscopic/molecular structure and order of the employed systems and their macroscopic properties and functions.

In this communication we will discuss first new improvements of the recently introduced electro-optical (EO-) waveguide microscopy[1, 2]. It is demonstrated that in

addition to the usual characterization of planar waveguide structures in terms of their (anisotropic) refractive index and thickness data[3] this technique allows for the visualization of lateral fluctuations of the poling efficiency and of the Pockels response while applying an electric DC field.

A promising new class of materials for EO-device applications are glassy solid polyelectrolytes (so-called Ionenes)[4, 5] with NLO active chromophores as counterions. A very high level of doping can be obtained without recrystallization of the chromophores[6], and various materials properties, e.g. the glass transition temperature Tg, can be tuned independently by choosing the appropriate polymer backbone. First EO-parameters obtained by ATR waveguide spectroscopy will be presented.

EXPERIMENTAL

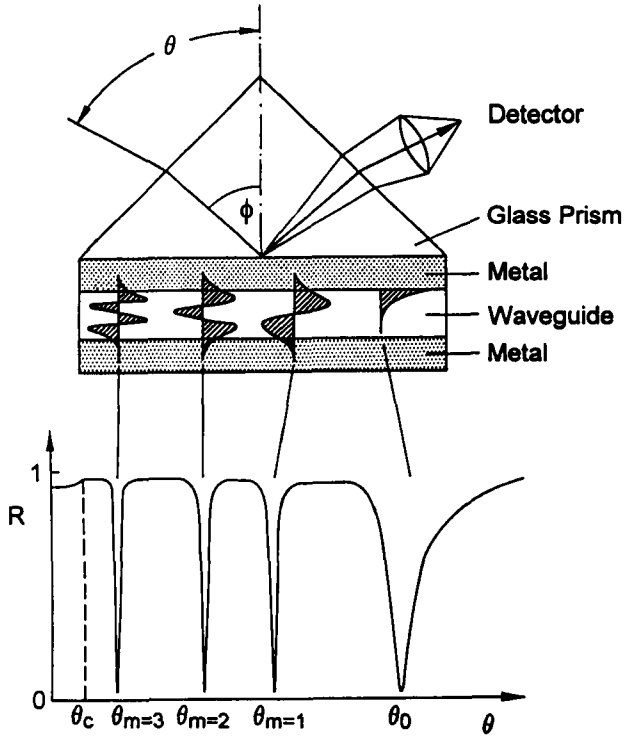

FIGURE 1: Schematic of the sample configuration used for waveguide analysis.

All linear and nonlinear optical (electro-optical) characterizations were performed with an experimental set-up designed for waveguide analysis based on the Kretschmann prism coupling technique[7, 8]. A schematic of this configuration is given in Figure 1. Onto the base of a glass prism (BK7 or LaSFN9 from Schott) first a thin layer (d ~ 40 nm) of Ag or Au is evaporated that defines on the one side the coupling gap needed for the excitation of waveguide modes and on the other side serves as an electrode for the poling procedure and for the Pockels measurements. The guiding material was a thin polymer film prepared by spin-casting.

Various polymer systems were employed for these investigations. The EO-waveguide microscopy was demonstrated with a thin spin-cast film of poly(methylmethacrylate) (PMMA) as host matrix and disperse red 1 (DR1) as the dissolved guest. The non-centrosymmetry in the orientation distribution of the chromophore needed for $\chi^{(2)}$-processes was achieved by electrode poling. For this purpose the top electrode was evaporated directly onto the polymer film, and the usual temperature-voltage-time procedure[13] applied.

The solid polyelectrolytes are materials based on a general chemical structure as given in Figure 2.

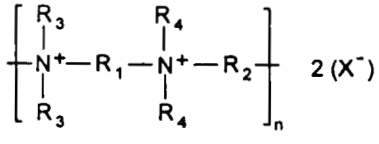

Ionene

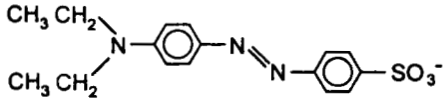

Ethylorangesulfonate

FIGURE 2: General structure formula of solid polyelectrolytes called ionene (X^- denotes the counter ion) and a nonlinear optically active chromophore ion ethylorange-sulfonate.

Their synthesis and basic materials' properties were described before[4, 5]. Doping with the $\chi^{(2)}$ active chromophore ethylorange sulfonate (cf Fig. 2) was achieved by an ion exchange reaction. Thin films could be prepared by spin-coating. The evaporation of the top electrode for the ionene systems, however, resulted in a critically enhanced surface roughness which prevented a reasonable waveguide analysis. Poling of these samples therefore was achieved by a corona discharge procedure.[9] The top electrode needed for the EO-measurements was evaporated onto another glass slide which was then mechanically pressed against the polymer film prepared at the base of the coupling prism.

Guided optical waves were identified by monitoring the reflected s- or p-polarized light from a HeNe laser (λ = 633 nm) as a function of the angle of incidence θ (R-versus-θ scan). Fresnel fit-calculations then yielded the (anisotropic) refractive index as well as the thickness, h, of the waveguide structure.[8]

Pockels coefficients were determined by applying an alternating voltage U (electrical field E typically 10V/μm) at a frequency of 2 kHz and recording the resulting reflectivity modulation with a lock-in detector. From these ΔR - versus - θ scans the electro-optical coefficients $\chi^{(2)}_{113}$ and $\chi^{(2)}_{333}$ as well as the piezo-coefficient ($\partial h/\partial U$) could be determined in the usual way[10, 11].

For the (electro-)optical waveguide microscopy of lateral heterogeneities of the various samples not only the specularly reflected light but also scattered and out-coupled waveguide light within a certain spacial frequency range was collected and focused onto a CCD camera[12]. Thus, images of the waveguide films could be obtained with a lateral resolution of a few μm. "Illumination" of the sample was possible with each of the guided modes, i.e., in particular, also with s- or p-polarized light.

In addition to these contour maps of the thickness and/or index topography of the planar waveguide films, images of the lateral variations of their Pockels response could be obtained by the following procedure: within the angular range of a particular guided mode pictures were taken at various angles (with an increment of typically 0.1 deg) with either no field applied or with a voltage of U = 100 V applied to the waveguide structure. For each pixel (field) this resulted in an intensity difference value the maximum of which (at a certain angle of incidence) gave a quantitative measure of the

local Pockels response. If plotted in a 2D-matrix an EO-efficiency map of the waveguide was obtained.

RESULTS AND DISCUSSION

Electro-optical waveguide microscopy

The examples presented here were obtained with a thin spin-cast film of PMMA as host material doped with 8% (weight/weight) DR1 as guest. The waveguide was sandwiched between two Ag electrodes and poled for 40 min at T = 80° C with U = 210 V. In order to demonstrate the sensitivity of the technique the sample was allowed to relax for 2 weeks, a time period during which most of the polar orientation of the chromophores decayed.

In order to evaluate the linear and nonlinear optical properties of the waveguide and to obtain first information about its film homogeneity over larger distances we recorded reflectivity R - as well as ΔR - scans at three different positions on the sample.

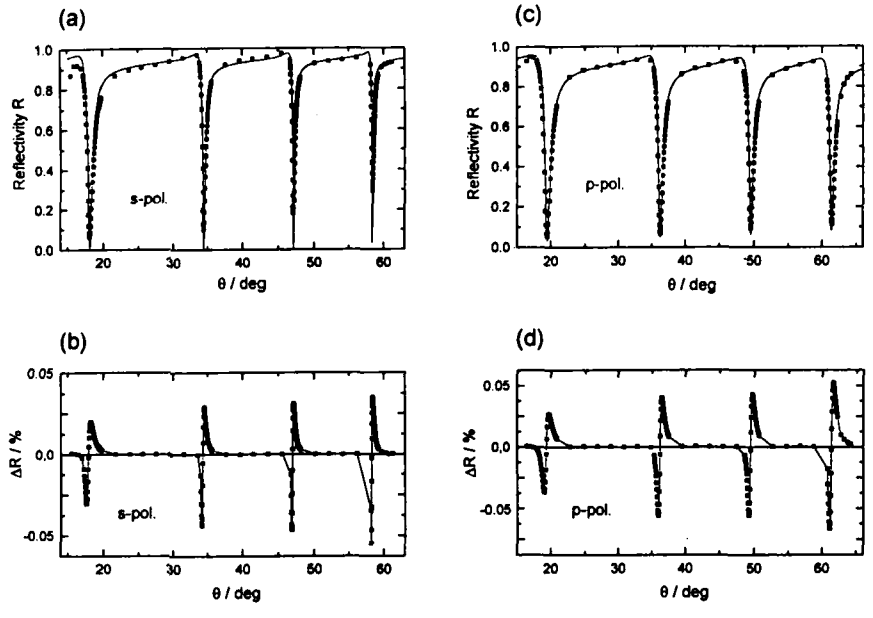

FIGURE 3: Reflecting R-versus-θ ((a) and (c)), and ΔR-versus-θ ((b) and (d)) scans.

Figure 3 gives the results for s- and p-polarization obtained for the angular range between $\theta = 15°$ and $\theta = 67°$ at sample position # 1 (cf also Fig. 5). The Fresnel fit curves of the R-versus-θ scans (full curves in Figs. 3(a) and (c), respectively) describe the experimental data rather well - an indication that the lateral heterogeneities of the sample within the area of the laser spot are rather moderate. As one can see from Table 1 which summarizes the thickness and the anisotropic (uniaxial) refractive index data obtained for the three different spots on the waveguide it is only the thickness that varies slightly across the film.

TABLE I Linear and nonlinear optical parameters of a PMMA/DR1 waveguide analysed by ATR-spectroscopy at 3 different spots on the sample

Spot #	ε_o'	ε_e'	h/ nm	$\chi_{113}^{(2)}$ / pm · V^{-1}	$\chi_{333}^{(2)}$ / pm · V^{-1}
1	2.292	2.302	2074.0	2.76	6.74
2	2.293	2.302	2084.6	2.23	7.00
3	2.292	2.302	2076.2	2.10	6.40

The electro-optic analysis of the ΔR-data (Figs. 3(b) and (d), respectively) indicate a larger lateral fluctuation of the Pockels coefficients (cf. Table 1).

A more detailed picture of the sample heterogeneities could be derived in a rather straight forward way by optical waveguide microscopy (OWM). Figure 4 gives a series of OWM micrographs taken with s-polarized light at different angles of incidence (as indicated) between $\theta = 18.0°$ and 18.9°, i.e., in the region of the m = 8 waveguide mode (cf Fig. 3(a)). In each of the pictures the areas of low intensity are at resonance at the corresponding angle of incidence and hence appear dark in reflection. A few details can be seen directly in these images: Two dust particles in the film (one in the center of the picture and one in the upper left corner) had a substantial impact on the flow of the polymer solution during the spin-coating step and resulted in a larger (local) thickness variation. The spot in the upper right area of the sample is a defect structure that originates from a current pulse applied during poling in order to heal an electrical short-cut at that spot.

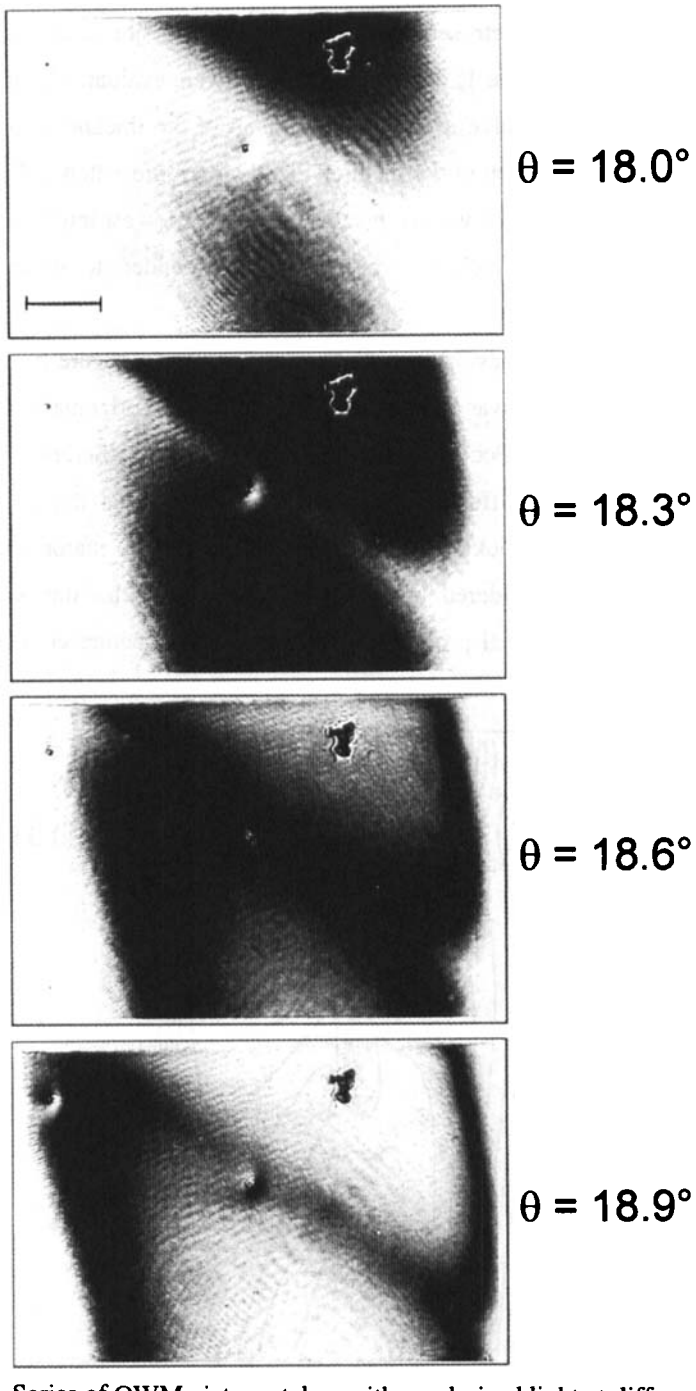

FIGURE 4: Series of OWM pictures taken with s-polarized light at different angles of incidence as indicated. The bar corresponds to 500 μm on the sample.

Since the waveguide spectroscopic scans indicated no major lateral variation of the refractive index data (cf. Table 1) the images of Fig. 4 were evaluated by image analysis computer routines so as to give a topographical map of the thickness variation of the polymer film. To this end each of the pictures like the ones presented in Fig. 4 were fed into the computer and analysed with respect to the lines of lowest intensity. The Fresnel calculation then gave the thickness value that corresponded to these lines at the respective angle of incidence.

The plot of all these lines-of-equal-thickness is given in Figure 5. (Note that the obtained topographical map was rescaled with respect to the horizontal coordinate so as to match to the scale of the Pockels map of Fig. 6 (see below).) Series of images taken with different modes and different polarizations confirmed that the dominant lateral variation is found for the thickness of the waveguide while no major refractive index fluctuations have to be considered. We should note, however, that this way also lateral variations of the linear optical properties of a waveguide structure could be evaluated quantitatively.

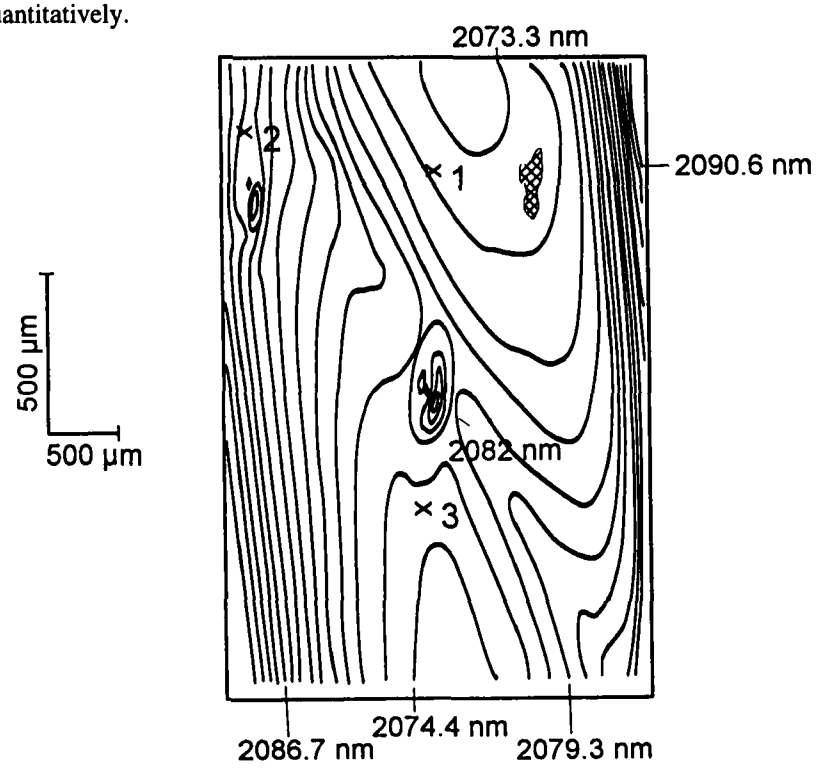

FIGURE 5: Topographical map of the PMMA waveguide.

If images are taken at different angles but each time not only in the absence of any voltage (as in the case of the micrographs presented in Fig. 4) but also after applying a constant electrical field of sufficient strength a slight difference in the intensity pattern of the two corresponding images mirrors the shift of the (local) resonance conditions induced by the index variation of the EO-active waveguide material. In principle, also electro-strictive thickness variations would contribute to the intensity changes but can be neglected for this DR1/PMMA sample.

For each pixel or pixel field the obtained intensity differences change with the angle of incidence in a characteristic way, as does the ΔR-curve in the usually applied EO-waveguide spectroscopy (cf. Figs. 3(b) and (d)), and see also Fig. 9(b) in ref. 12). The maximum amplitude of this difference intensity variation is a measure of the local Pockels response of the poled polymer film to the applied field. A 2D-plot of these local maximum values, therefore, represents a map of the lateral variation of its EO-activity.

FIGURE 6: EO-activity map of the same waveguide as shown in Fig. 5.

Figure 6 gives the result of such an analysis at a reduced spatial resolution based on a matrix of 24 x 18 pixel fields (each averaging 25 x 25 pixels). Since this analysis was based on OWM images taken with p-polarized light at an angle of incidence near θ = 73°, i.e. with the m = 4 mode, the size of the sample area imaged on the camera is substantially larger than the one given in Fig. 4 also including parts of the polymer film not covered by the top electrode. These areas were not poled and hence showed also no EO-efficiency but rather appeared dark in the ΔR-images. This can be clearly seen in Fig. 6 in the upper narrow dark stripe and in the area at the upper right corner. Also the burned defect was electro-optically dead and appeared dark. Clearly seen are also the two dust particles with their surrounding halo of reduced EO-efficiency.

In addition to these local variations of the Pockels coefficients near structural singularities there exists also a larger gradual variation of the EO activity, even on rather smooth film areas. The maximum variation seen in the flat regions of Fig. 5 amounts to about 40% which has to be compared to a thickness variation of only about 1%. These substantial variations of the EO-response therefore cannot be explained by lateral variations of the field strength during poling or during the ΔR-measurement but rather have to be linked to other structural parameters that vary laterally and influence the poling efficiency. (Note that the rather small variations of the EO-coefficients obtained for the 3 different spots on the sample by EO waveguide spectroscopy presented in Table 1 mirror the fact that by choice the three locations analysed were in areas of similar activity.)

We should point out that the qualitative information about lateral fluctuations of the linear optical properties of polymer waveguides (including thickness variations) could be derived from OWM images in a rather straightforward way. Similarly, ΔR-images gave a direct qualitative picture of EO-efficiency variations across the planar waveguide. Even the semiquantitative analysis of the data - at least in terms of a relative efficiency map across the waveguide - was easily possible because this polymeric host/guest-system has only a negligable piezo-response and the net effect of an applied DC field to the optical response probed by a p-polarized mode is dominated by the $\chi^{(2)}_{333}$ coefficient of the $\chi^{(2)}$ tensor. Thus, a single set of ΔR-images taken at different angles of incidence was sufficient for the generation of the map presented in Fig. 6.

But even in the case where all the other response coefficients cannot be ignored and contribute to the local net effect though, in general, in a laterally varying way, the full analysis, in principle, can be performed. It then requires, however, the correlated evaluation of several series of pictures taken with different polarizations (probing different $\chi^{(2)}$ - tensor components) and with different waveguide modes (mixing Pockels- and electro-strictive responses in a different way).

Solid polyelectrolytes as EO-active waveguides

A recently introduced class of glassy polymers, called ionenes, with promising optical properties is based on the general structure given in Figure 2. By the variation of the ammonium substituents, and in particular, by a careful choice of the polymer backbone components R_1 and R_2, a tailor-made profile of general polymer properties can be designed. E.g., the glass transition temperature could be shown to vary from T = -20°C up to T = 200°C. The choice of the counterions X^- largely determines the optical properties. This has been used, e.g., to synthesize glassy polymers with rather high refractive indices, yet with a relatively low dispersion, i.e., high Abbé number.[5)]

If charged NLO-active chromophores were introduced as counterions also high nonlinearities could be obtained. For a $\chi^{(3)}$-active system it could be shown that even very high volume fractions of up to 69% could be prepared for such a simple host/guest-system[6)] with long term stability because the electrostatic interaction between the host matrix and the guest chromophore prevents the dye from recrystallization.

We present here first examples of a $\chi^{(2)}$-active ionene system based on a polymer with $R_3 = R_4 = CH_3$, $R_1 = (CH_2)_6$, and $R_2 = (CH_2)_{10}$. X^- was ethylorangesulfonate the structure of which is also given in Figure 2.

The good waveguide forming properties of ionenes had been demonstrated before[5)] and were also found for the ion exchanged material. Waveguide mode pattern obtained with s- and p-polarized light even after evaporation of the top gold electrode showed excellent agreement with Fresnel fit calculations. However, the electrode poling process, though possible to a certain degree by optimizing the temperature - voltage - time protocol of the process, resulted in a substantial loss of the waveguide quality with only very broad resonances in the reflectivity scans. Already by eye the surface roughening could be seen.

We therefore choose a different approach. After spin-coating the material onto the Au-coated substrate a corona discharge was applied in order to pole the chromophores in the waveguide film. The top electrode required for the EO-measurements was then first evaporated onto a separate glass slide and subsequently mechanically pressed against the poled polymer film. The resulting reflectivity scans are shown in Figure 7(a) for s-polarized excitation and in Figure 7(c) for p-polarization, respectively.

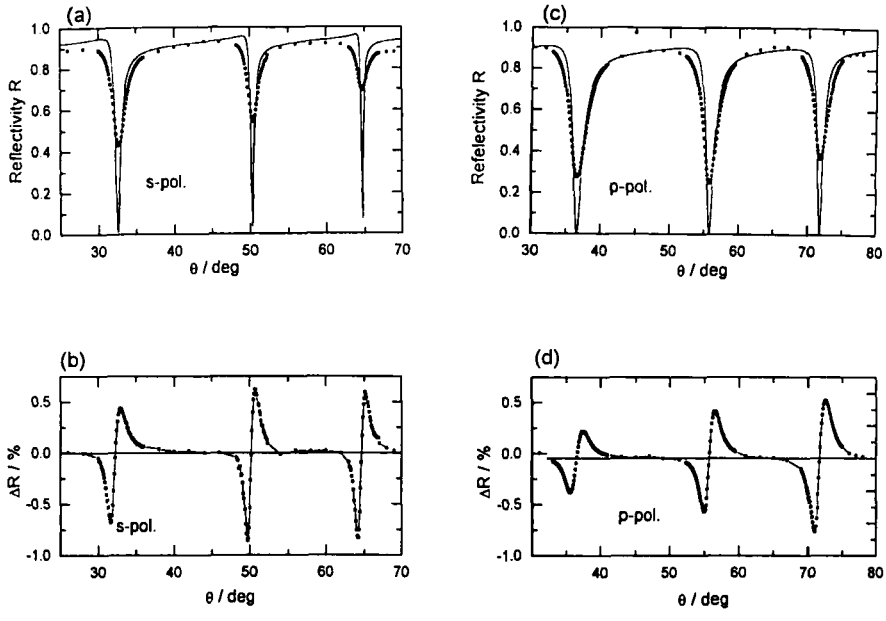

FIGURE 7: Reflectivity R-versus-θ ((a) and (c)), and ΔR-versus-θ ((b) and (d)).

As judged immediately from the weak and broad waveguide resonances substantial scattering losses limit the coupling efficiency. Despite this however, a Fresnel fit calculation allows for the determination of the optical anisotropy of the poled film and gives $\varepsilon_0' = 2.877$ and $\varepsilon_e' = 2.904$, as well as the thickness of the film, $h = 1205.8$ nm. The weak birefringence induced by the corona poling indicates that this process was rather ineffective.

Nevertheless, ΔR-scans could be obtained and are shown for s- and p-polarization in Figures 7(b) and (d), respectively. The response coefficients that were derived by the usual analysis[11] are

$\chi^{(2)}_{113}$ = 17.2 pm/V

$\chi^{(2)}_{333}$ = 49.5 pm/V

$\partial h/\partial U$ = - 0.77 pm/V

The piezo-response of this material is 1 - 2 orders of magnitudes smaller than the Pockels coefficients and hence can be neglected. The electro-optical coefficients are certainly slightly resonance enhanced at λ = 633 nm but, nevertheless, are rather promising. Moreover, because the described experiments and procedures were the very first ever performed with these ionene polymers there should be room for further substantial improvements. We note, in particular, that the recently introduced all-optical poling under the influence of the simultaneous irradiation of the sample with a fundamental and a (phase coherent) second harmonic beam [13, 14] should be the technique of choice because problems arising from the intrinsic conductivity of this material should be of no importance.

REFERENCES

§ This contribution is the shortened version of a paper presented at the 2nd Mediterranean Workshop and Topical Meeting on Novel Optical Materials and Applications - NOMA in Cetraro/ Italy, May 28 - June 2, 1995.

1. E.F. Aust and W. Knoll, J. Appl. Phys., 73, 2705 (1993).
2. E.F. Aust, W. Hickel, H. Knobloch, H. Orendi, and W. Knoll, Mol. Cryst. Liq. Cryst., 222, 49 (1993).
3. W. Hickel and W. Knoll, Appl. Phys. Letters, 57, 1286 (1990).
4. H.-U. Simmrock, A. Mathy, C. Dominguez, W.H. Meyer, and G. Wegner, Angew. Chem. Adv. Mater., 101, 1148 (1989).
5. A. Mathy, H.-U. Simmrock, and C. Bubeck, J. Phys. D: Appl. Phys., 24, 1003 (1991).
6. W.A. Meyer, J. Pecherz, A. Mathy and G. Wegner, Adv. Mater., 3, 153 (1991).
7. E. Kretschmann and H. Raether, Z. Naturforsch., 23a, 2135 (1968).
8. E.F. Aust, S. Ito, M. Sawodny, and W. Knoll, TRIP, 2, 313 (1994).
9. R.H. Page, M.C. Jurich, B. Reck, A. Sen, R. Twieg, J. D. Swalen, G.C. Bjorklund, and C.G. Willson, J. Opt. Soc. Am., B7, 1239 (1990).
10. M. Dumont, Z. Sekkat, D. Morichère, and Y. Levy, Accurate Measurements of Thin Films Index Variations, SPIE Proceedings, Vol. 1559, 127 (1991).

11. D. Morichère, Etude des Propietés Electrooptiques de Couches Minces Organiques par la Méthode de la Reflexion Totale Attenuée, PhD Thesis, Université de Paris-Sud, Centre d'Orsay, Paris (1991).
12. E.F. Aust, M. Sawodny, S. Ito, and W. Knoll, Scanning, 16, 353 (1994).
13. F. Charra, F. Kajzar, J.M. Nunzi, P. Raimond, and E. Idiart, Optics Letters, 18, 941 (1993).
14. J.M. Nunzi, F. Charra, C. Fiorini, and P. Raimond, Mol. Cryst. Liq. Cryst., 225, 85 (1994).